Received January 7, 2022, accepted January 25, 2022, date of publication January 28, 2022, date of current version February 10, 2022.

Digital Object Identifier 10.1109/ACCESS.2022.3147589

7 T Niobium-Titanium-Based Persistent-Mode Superconducting Magnet for an Electron Beam Ion Source

SU-HUN KIM[1], (Member, IEEE), DIPAK PATEL[2], YEUNDAE JEONG[3], MINHEE KIM[4], SE-HEE LEE[4], JUNG HO KIM[5], AND SEYONG CHOI[6]

[1]Department of Electrical Engineering, Kyungpook National University, Daegu 41566, Republic of Korea
[2]School of Mechanical and Mining Engineering, The University of Queensland, St. Lucia, QLD 4067, Australia
[3]KR Tech, Dong-gu, Daegu 41059, Republic of Korea
[4]School of Electronic and Electrical Engineering, Kyungpook National University, Daegu 41566, Republic of Korea
[5]Institute for Superconducting and Electronic Materials, Australian Institute for Innovative Materials, University of Wollongong, Squires Way, Innovation Campus, North Wollongong, NSW 2500, Australia
[6]Department of Electrical Engineering, Kangwon National University, Kangwon 25914, Republic of Korea

Corresponding authors: Jung Ho Kim (jhk@uow.edu.au) and Seyong Choi (syc@kangwon.ac.kr)

This work was supported by the Basic Science Research Program through the National Research Foundation of Korea (NRF) funded by the Ministry of Education under Grant 2020R1A6A3A01100198.

ABSTRACT A high field magnet is a key element of cryogenic electron beam ion sources (EBISs), which are known for generating highly charged ions through the magnetic compression of an electron beam. Herein, we report the design, fabrication, and evaluation of a 7 T niobium-titanium superconducting magnet capable of persistent-mode operation. The magnet was designed using finite element analysis by considering its magnetic, thermal, and mechanical properties. The designed magnet was then fabricated, assembled, and evaluated for various design parameters in a recondensing-type liquid helium cryostat. After several quench trainings, the magnet reached a target magnetic field of 7 T with an operating current of 200 A, a magnetic field uniformity of 0.24%, and an electron beam focusing length of 1.3 m inside the bore. The magnet was successfully operated in the persistent-mode for 9.5 days (228 hours) and achieved a field-decay rate of 0.42 ppm $\cdot$ h^{-1}. The magnet evaluation results confirm that our superconducting magnet system can be applied to an EBIS to carry out stable and effective electron beam compression.

INDEX TERMS Niobium-titanium magnet, persistent-mode operation, persistent current switch, electron beam ion source, finite element method.

I. INTRODUCTION

An electron beam ion source (EBIS) is known for producing highly charged ions (HCIs) [1]–[6]. To create a high-density electron that improves the quality of HCIs, it is essential that the electron beam focusing is present within an EBIS [1], [7], [8]. A sufficiently strong and uniform magnetic field is functionally required, therefore, for focusing the electron beam within an EBIS [3], [9]–[11]. Two types of EBIS exist: a room-temperature EBIS, in which the magnetic field is generated using permanent magnets and a cryogenic EBIS, in which the magnetic field is generated using a superconducting magnet.

The associate editor coordinating the review of this manuscript and approving it for publication was Asif Islam Khan.

In cryogenic EBISs, a niobium-titanium (Nb-Ti) based liquid helium (LHe) cooled superconducting magnet generates a strong and uniform magnetic field, which efficiently focuses the electron beam [2]. Alessi *et. al.* reported a 5 T superconducting magnet for an EBIS manufactured by ACCEL Instruments GmbH (now Bruker Advanced Supercon GmbH) [12]. The magnet had features of a warm bore of 204 mm, a length of 2 m, and a field uniformity of $\pm$0.5% over the trap length of 1.5 m. Kondrashev *et. al.* also reported a 6 T superconducting magnet for an EBIS [13]. The magnet had a warm bore of 155 mm and a length of 1 m [14]. In addition, J. Zhu *et. al.* reported a 4.5 T superconducting magnet for an electron beam ion trap with the persistent-mode operation [15]. The magnet had a warm bore of 75 mm, a length of 75 mm, and a field homogeneity of $\pm$200 ppm over the trap length of 20 mm.

In recent years, the price of LHe continuously increased, and this trend is expected to continue [16]–[18]. Therefore, to minimize the need to frequently refill the cryostat of the superconducting magnet, developing a recondensing-type LHe cryostat for an EBIS system is highly desirable [19]. Recently, a 5 T superconducting magnet was developed and installed in an LHe recondensing-type cryostat for an EBIS at Brookhaven National Laboratory [20], [21]. The magnet exhibits features of a warm bore of 215 mm, a length of 2.3 m, and a field uniformity of ±0.5% over the trap length of 1.5 m. To further improve the performance of an EBIS such as the smaller electron beam radius, however, an Nb-Ti magnet with a higher magnetic field and spatial uniformity is required [3]. Because the high inductance of the magnet for EBIS causes a long current charging time, it is necessary to improve the operation efficiency by applying the persistent-mode. If an Nb-Ti magnet also adopts the persistent-mode in an LHe recondensing-type cryostat, it would considerably reduce the operational cost of the system and the heat input into the cryostat [18], [19], [22].

In the present study, we design, fabricate, and evaluate a 7 T Nb-Ti based persistent-mode superconducting magnet for an EBIS. Our magnet exhibits a warm bore of 204 mm, a length of 2 m. Also, depending on the operating time and beam physics, field-decay rate of less than 1 ppm $\cdot$ h^{-1} and field uniformity of below ±0.3% over a trap length of 1.3 m were required. We evaluate the performance and cross-section of the procured Nb-Ti wire. By considering the performance of the wire, the coil is designed and analyzed with a focus on magnetic field uniformity and the distribution of radial and hoop stresses within the winding pack. The switching times of persistent current switch (PCS) are estimated using finite element analysis (FEA). Following the design, both the magnet and PCS are fabricated using the wet winding method. Finally, the transport current, field uniformity, and persistent-mode capability of the fully assembled magnet are systematically evaluated.

II. NIOBIUM-TITANIUM SUPERCONDUCTING WIRE FOR AN ELECTRON BEAM ION SOURCE

A rectangular multifilament Nb-Ti/Cu (copper) wire for winding the magnet was procured from Luvata [23]. The rectangular wire was selectively chosen to improve the filling factor of the winding pack. First, the transverse cross-section of the wire was observed using an optical microscope, as shown in Fig. 1(a). The formvar insulated wire measured 1.4 × 0.95 mm. The wire exhibited 78 inner filaments (each 80 μm in diameter), a 2.4:1 ratio of Cu to superconductor, and a Young's modulus of ∼100 GPa (<100 K). To observe the selected area of the wire more closely, the detailed scanning electron microscopy (SEM) was also carried out. The SEM image of the selected area of the wire is shown in Fig. 1(b), along with the corresponding electron dispersive X-ray spectroscopy (EDS) element maps and line spectrums of one of the filaments. As can be seen in Fig. 1(b), the filaments

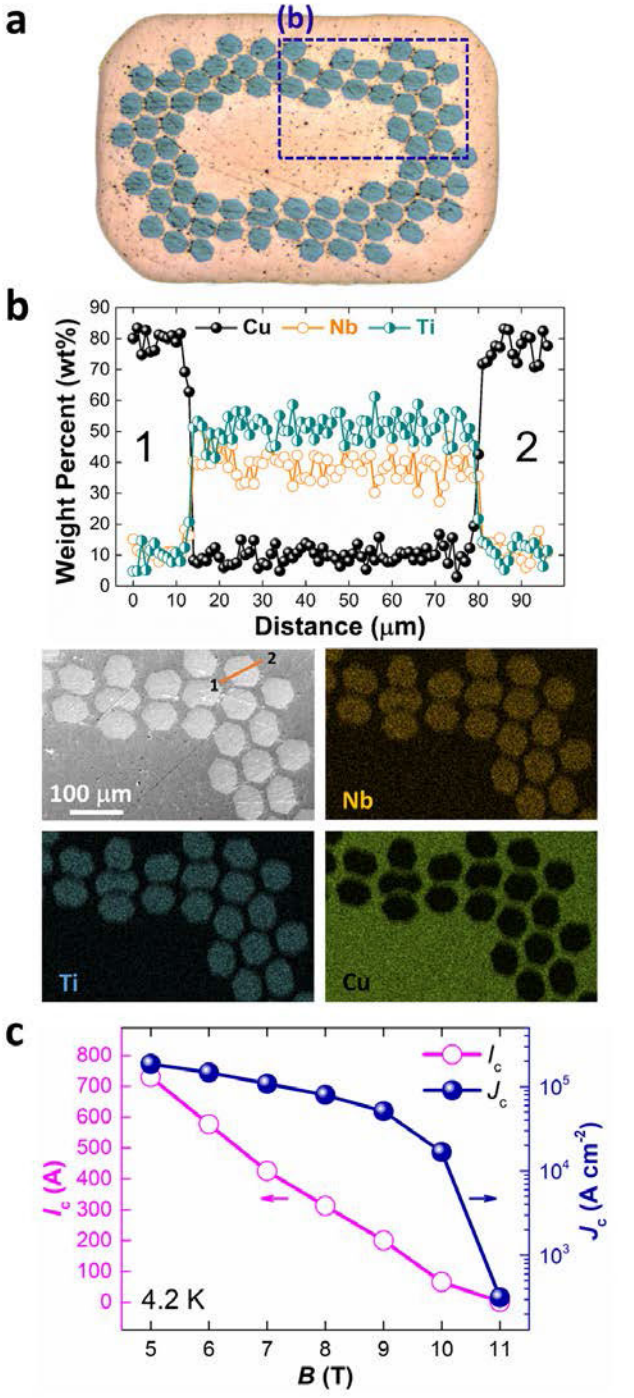

FIGURE 1. (a) Transverse optical cross-sectional image of the multifilament Nb-Ti/Cu wire, (b) SEM image of the selected area of the wire, along with the corresponding EDS element maps and line spectrums of one of the filaments, and (c) I_c and J_c versus magnetic field characteristics of the Nb-Ti/Cu wire at 4.2 K.

were composed of Nb-Ti/Cu, and the matrix material was pure Cu.

Next, the critical current (I_c) of the Nb-Ti/Cu wire was measured in different magnetic fields at 4.2 K with an electric field criterion of 0.1 μV $\cdot$ cm^{-1}, as shown in Fig. 1(c). Based

on the I_c values, the corresponding critical current density (J_c) was also calculated. The I_c of the wire in the 7 T at 4.2 K was estimated to be 425 A, whereas, in 8 T, it was 312 A. The magnet was designed based on the wire performance.

III. DESIGNING THE NIOBIUM-TITANIUM SUPERCONDUCTING MAGNET FOR AN ELECTRON BEAM ION SOURCE

A. NIOBIUM-TITANIUM MAGNET DESIGN

The superconducting magnet design aimed to meet the required electron beam focusing length of 1.3 m with a 7 T field and a field uniformity of <0.3% in the length along the central axis of the magnet. In this design, some design parameters were predetermined to assemble other pre-built accelerator components and beamline. Hence, the inner diameter (ID) and length of the magnet were fixed at 276 mm and 2 m, respectively. The thickness of the magnet bobbin was designed to be 8 mm to sufficiently withstand the mechanical stresses generated under the cryogenic and high magnetic field environments. The operating current was limited below 250 A. By considering these constraints, we designed the Nb-Ti superconducting magnet for an EBIS, as shown in Fig. 2. To adhere to the magnet's required design parameters, our design included a main coil and a set of correction coils, and the detailed design parameters are shown in Table 1.

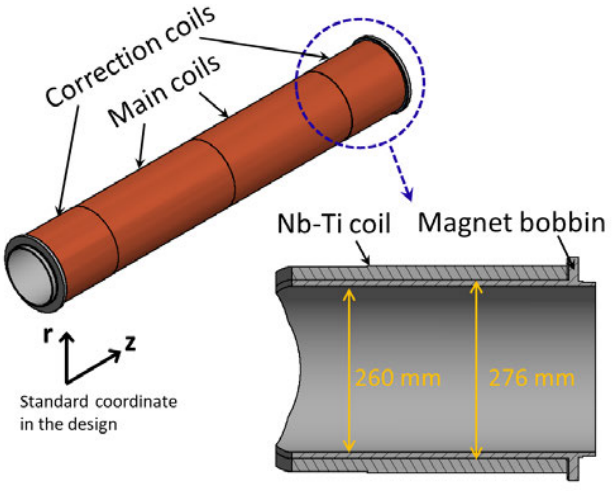

FIGURE 2. Schematic diagram of the designed 7 T Nb-Ti superconducting magnet with standard coordinate in the design.

The magnetic field and structural stability of the designed superconducting magnet were evaluated by finite element analysis based on Table 1. The thermal stability can be evaluated with the temperature margin, which is estimated by the operating point on the straight line for the critical temperature and critical current [24]. In our designed magnet, the temperature margin was ~2 K. The surface plot of the magnetic flux density norm of the magnet is shown in Fig. 3(a). As can be seen in the figure, the peak field in the magnet was calculated to be 7.1 T. Fig. 3(b) shows magnetic field density versus axial distance (z-axis) plots of the designed and deformed (thermal and magnetic stresses combined) model. As can be seen Fig. 3(b), the magnetic field was maintained without field distortion due to deformation. The magnetic field uniformity was calculated by $(B_{max}-B_{min})/(B_{max}+B_{min})\times 100\%$. The field uniformity along the beam focusing length was estimated to 0.24%, which is still within the required field uniformity of ±0.3% over a trap length of 1.3 m.

TABLE 1. The design parameters of the Nb-Ti superconducting magnet for an EBIS.

Parameters		Values
Magnetic field at the magnet center (T)		7.01
Peak field in the winding pack (T)		7.10
Beam focusing length (m)		1.30
Uniformity of magnetic field along the beam focusing length (%)		0.24
ID of the coils (mm)		276
OD of the coils (mm)	Main coil	348.2
	Correction coils	352
Length of the coil (m)		1.99
Turns/layers	Main coil	818/38
	Correction coils	302/40 (1 pair)
Coil current (A)		207.5
Current margin (%)		51.18
Total conductor length (km)		54.4
Operating temperature (K)		4.2
Temperature margin (K)		~2
Magnetic stored energy (MJ)		2.75
Inductance (H)		127.5

A superconducting magnet is known to suffer from magnetic stress (called the Lorentz force) and, in cryogenic environments, thermal stress [24]–[26]. To ensure the mechanical stability of the solenoid, estimating the total combined stress (thermal and magnetic) was thus necessary. In the designed solenoid model, stainless steel (SS) tension wire was banded to the outside of the solenoid to improve mechanical stability. The mechanical stress and stability in the solenoid magnet depending on the tension wire were estimated using magnetic-thermal-structural FEM analysis. Fig. 4 shows the radial and hoop stress distributions for the r-axis direction at the center and at 350 and 750 mm along the z-axis in the solenoid. Also, these results were compared with and without SS tension wire. In Fig. 4(a), it can be seen that the radial stress distribution was compressive and applying the tension wire acts to contract more in the radial direction. Moreover, a solenoid magnet swells under the magnetic field due to the Lorenz force (hoop stress). Fig. 4(b) shows the hoop stress that acts on the circumferential direction of the winding with and without tension wire. The hoop stress was reduced with the tension wire, and its values were significantly lower than the yield strength of the Nb-Ti, which is ~310 MPa at 4.2 K [27]. This estimation indicates that the solenoids were mechanically more stable with SS tension wire.

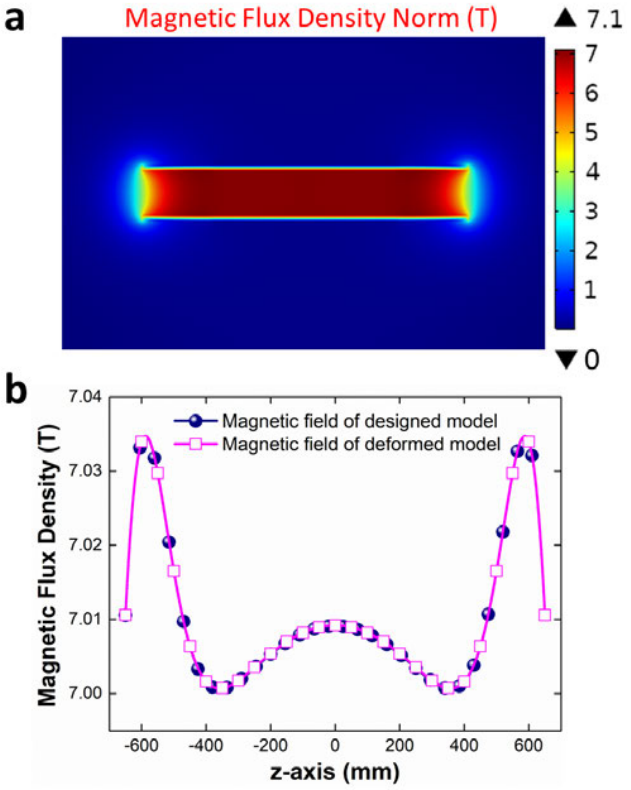

FIGURE 3. (a) Surface plot of the magnetic flux density norm of the magnet and (b) magnetic field density versus axial distance plots of the designed and deformed (thermal and magnetic stresses combined) model.

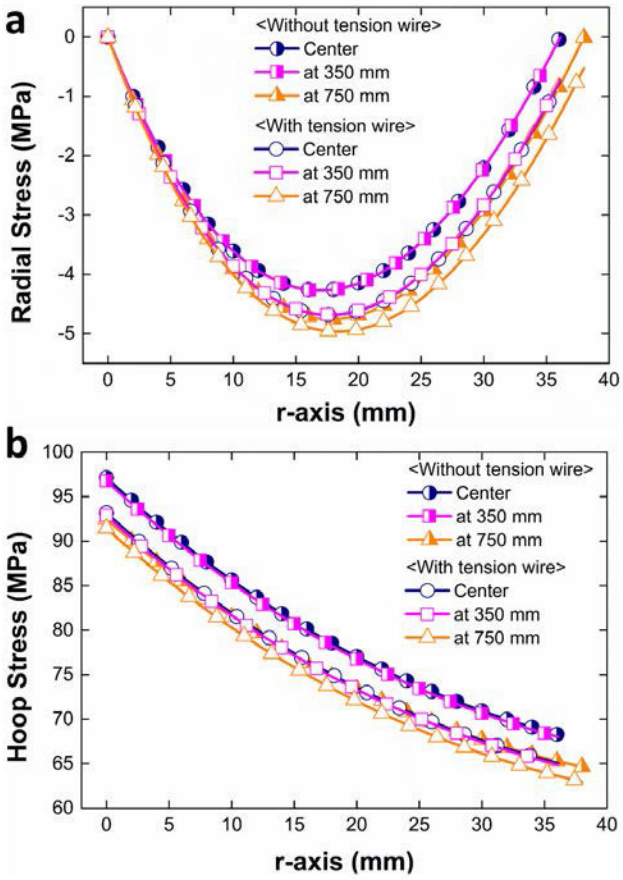

FIGURE 4. Estimated mechanical stress results according to applying the tension wire in the designed solenoid; (a) radial stress, and (b) hoop stress in the radial direction at the center and at 350 and 750 mm of the coil in length.

B. PERSISTENT CURRENT SWITCH DESIGN AND FABRICATION

Due to the high inductance of the magnet, its operation efficiency is low with slow current ramping rate. To overcome this issue, the persistent-mode operation was applied to our magnet. By considering operating period in EBIS system, the field-decay rate in persistent-mode limited ppm $\cdot$ h^{-1} (1μT decay per hour). For this operation, we designed PCS to make closed-loop with Nb-Ti magnet. The operation of designed magnet was predicted with a current ramping rate of 0.02 A.s^{-1} and a power supply with a compliance voltage of 2.5 V. By considering these parameters, the PCS was designed with a 7.44 Ω resistance at 20 K to restrict the maximum leakage current to 0.17%. Nb-Ti/Cu-Ni (copper-nickel) wire has higher electrical resistance in a normal state than Nb-Ti/Cu wire [28], [29]. This means that Nb-Ti/Cu-Ni provides a smaller PCS coil and effectively limits the leakage current to the PCS. Thus, the Nb-Ti/Cu-Ni wire was used to design and fabricate the PCS. The PCS wire had a diameter of 0.57 mm including an insulation of 0.07 mm, a resistivity of 1.24 Ω.m^{-1} at 20 K, and an I_c of 300 A in 3 T at 4.2 K. The PCS was installed away from the high field region to minimize the influence of the magnetic field. The total required conductor for the PCS was approximately 6 m in length. The designed PCS demonstrated an ID, outer diameter (OD), and height of 30, 33, and 18 mm, respectively. To make the PCS resistivity to charge the main magnet, a nichrome wire heater was wound inside the PCS coil. The heater wire had a diameter of 0.203 mm and an electrical resistivity of 33.2 Ω.m^{-1}. To generate 1.48 W of heating power with a 110 mA heater current, the required length of the heater was ∼3.67 m, and the total resistance was 121.89 Ω.

Fig. 5 shows the rationally designed PCS and its schematic diagram. As can be seen in Fig. 5(a), Nb-Ti/Cu-Ni and nichrome wires were wound around the G10 structure. For thermal insulation, Teflon was used on the outside of the Nb-Ti/Cu-Ni winding. An aluminum cover was designed to house the PCS for the rapid switching operation. The PCS temperature behavior was predicted by FEA, as shown in Fig. 5(b). As can be seen in the figure, we estimated that it would take 75 sec for the PCS to reach 20 K from 4.2 K after the heater was turned on; we estimated that it would take 125 sec for the PCS to cool down to 4.2 K after the PCS heater was turned off.

C. MAGNET MANUFACTURING

Based on our magnet design, we manufactured an Nb-Ti superconducting magnet for an EBIS, as shown in Fig. 6(a).

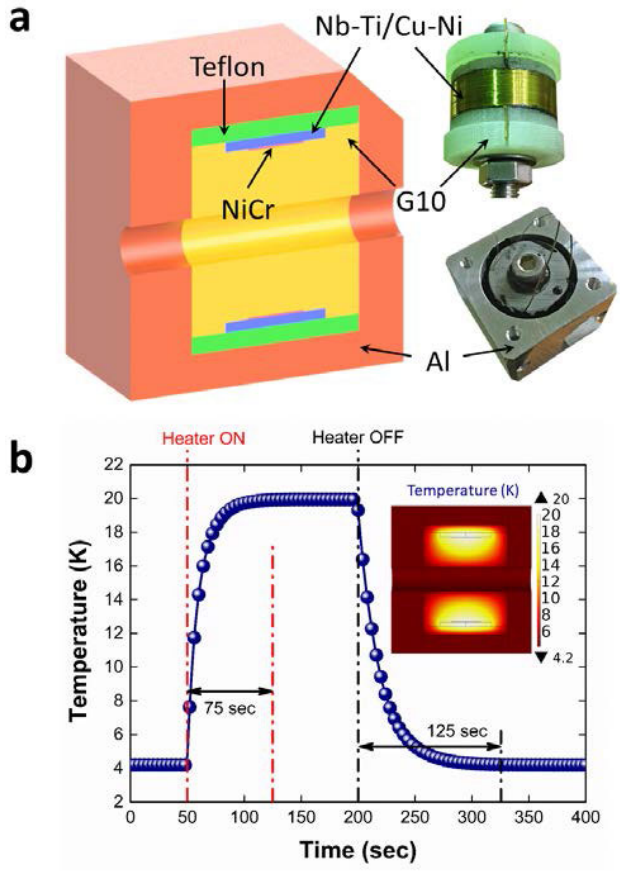

FIGURE 5. (a) Manufactured PCS and its schematic diagram and (b) estimated operation property of the PCS using thermal analysis.

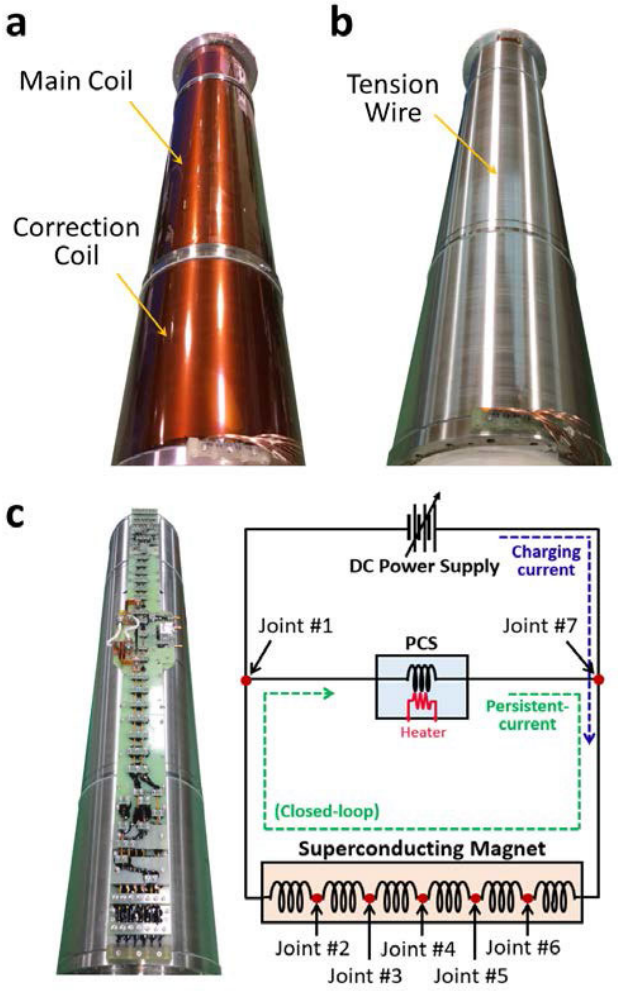

FIGURE 6. (a) Manufactured Nb-Ti superconducting magnet, (b) mechanically reinforced Nb-Ti magnet using the tension wire, and (c) electrical components and circuit diagram of the magnet system.

The center part was composed of the main coil for the 7 T center field, and the end parts were composed of correction coils. For the coil winding, a wet winding method was used with Stycast insulation between wires. The Lorentz force in a solenoid coil causes an expanding strain. To reinforce this issue, the SS tension wire was wound on the outside of the coil, as shown in Fig. 6(b). Fig. 6(c) shows electrical components such as PCS (for persistent-mode operation), diodes (for coil protection), and Nb-Ti superconducting joints, as well as the corresponding electrical circuit diagram of the entire magnet system. For quench protection, as a passive method, adiabatic using the copper matrix of Nb-Ti wire, and cold diodes of 3.5 V were connected in parallel with both ends and the center tap of the coil. Specifically, five superconducting joints were applied to connect the magnet coils, and two joints were utilized to make a closed circuit between the PCS and the magnet. Our superconducting joint technology has been reported in a previous study [22].

IV. OPERATION TEST OF 7 T NIOBIUM-TITANIUM SUPERCONDUCTING MAGNET

To evaluate the performance of the assembled magnet, a recondensing-type LHe cryostat was designed as shown in Fig. 7(a). It mainly consists of a vacuum chamber, a thermal shield, and a helium vessel. The LHe capacity of the cryostat was designed to be 400 L for cooling the superconducting magnet. To prevent any heat transfer, the thermal shield and helium vessel were floated by using Kevlar on the support link. In addition, Multilayer insulation was wrapped around the exterior of the thermal shield and the helium vessel. We reported our recondensing-type LHe cryostat design and thermal analysis previously [19]. From the reported results, the heat loads by conduction, radiation, and Joule heat were 46 W and 0.614 W, respectively, in the thermal shield and the helium vessel. For these, a couple of two-stage Gifford-McMahon cryocoolers with a cooling capacity of 1.5 W at 4.2 K and 45 W at 50 K were installed in the cryostat. Resultantly, the stable operation of the cryostat is expected with cooling margins of 48.9% and 79.5%. Fig. 7(b) shows manufactured recondensing-type LHe cryostat. As can be seen in the figure, high temperature superconductor (HTS) current leads, LHe ports, and recondensing units (including two Gifford-McMahon cryocoolers) were located at the

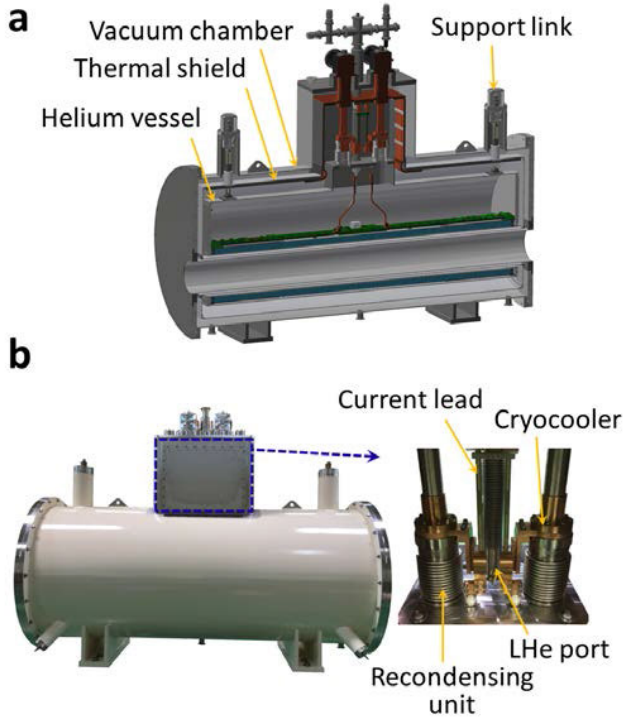

FIGURE 7. (a) Schematic diagram of a recondensing-type LHe cryostat and (b) assembled 7 T superconducting system developed for an EBIS.

upper center part. Once the magnet was cooled by the cryogen injected through the LHe port, the current was applied through the HTS current leads. During magnet operation, the heat loads were directly generated by conduction, radiation, and Joule heat, resulting in LHe vaporization. This vaporized LHe was then recondensed to minimize losses and improve cooling cost efficiency for practical operation. For the operation test of the superconducting system, a total of 12 temperature sensors were placed at the top and bottom of the coil, cold heads of cryocoolers, HTS current leads, helium vessel inner wall, and thermal shield inner wall. In addition, two LHe level sensors were installed on the edge of the inner wall of the helium vessel.

A low-temperature superconducting magnet designed for very high currents requires extensive quench training to enable the magnet to function at its full targeted currents [30]. Fig. 8(a) shows coil current and magnetic field versus quench training number plots for the assembled magnet. As can be seen in the figure, after five times intended "quench training", an operating current of 200 A and magnetic field of 7 T were reached in our magnet. Once the assembled magnet reached the target operation condition, it was stably operated without the quench. After that, the magnet was further evaluated for its magnetic field distribution and uniformity. This test was one of the important milestones of the successful design and fabrication of our magnet system because, as mentioned earlier, field strength and uniformity in an EBIS are important for effective electron beam compression. To evaluate these parameters (field strength and uniformity),

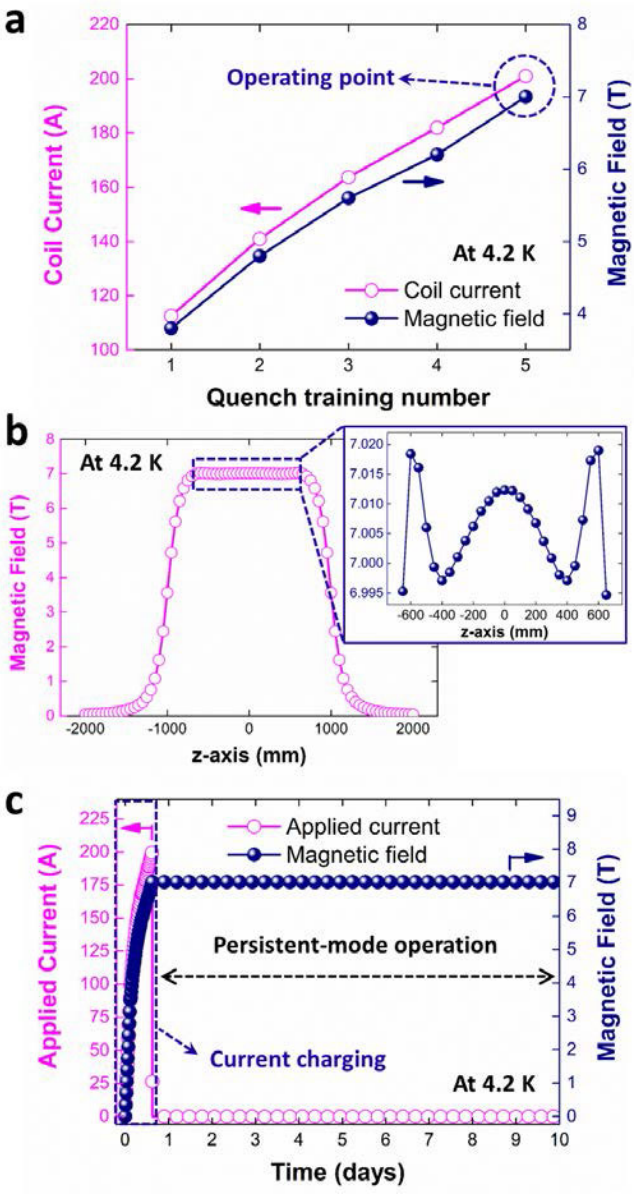

FIGURE 8. (a) Quench training history plot for the developed system during the test, (b) measured magnetic field distribution according to the axial line in the solenoid, and field distribution in the beam compression region (inset), and (c) the result for the 9.5-day test (excluding the charging time) of the magnet in persistent-mode.

the assembled magnet was tested at 4.2 K. In this test, the temperature and the magnetic field were acquired by using cryogenic temperature and Hall sensors, respectively. A real-time data was recorded by using LabVIEW software. For field uniformity, magnet field distribution was acquired along the z-axis with intervals of 50 mm by mounting a Hall sensor on the x-y-z position stage. Fig. 8(b) shows measured magnetic field distribution along the z-axis. The inset figure in Fig. 8(b) shows the field distribution in the electron beam compression region. The measured field uniformity was 0.24% at a 7 T magnetic field.

The persistent current is circulated in the closed circuit between the magnet and the PCS. For field-decay measurement, a Hall sensor, which is located at center of the magnet, detected the magnetic field generated by the persistent current. Fig. 8(c) shows the result of the persistent-mode operation. The magnet was operated in the persistent-mode without the externally applied current for approximately 228 hours (9.5 days), excluding the current charging time. The magnet remained stable at the 7 T field, with a field-decay rate of approximately 0.42 ppm · h-1 (61 nT decay per hour). The field decay caused by the *n*-value factor was negligible, since the charging current of 200 A was only 47% of the coil's critical current at 7 T [31]. As a result, we confirmed that our system can offer stable, long-term operation without any external current source.

V. CONCLUSION

A 7 T Nb-Ti based superconducting magnet capable of persistent-mode operation was successfully designed, manufactured, and evaluated for EBIS application. In the design phase, various numerical analyses were carried out to evaluate the magnetic, thermal, and mechanical stabilities in terms of magnet operation. The magnet was designed so that it met the required materials strength and magnetic field uniformity even after structural deformation. Based on the design, the magnet coils, PCS, and superconducting joints were separately manufactured and assembled. Finally, the magnet was installed into a recondensing-type LHe cryostat. The magnet attained a target field of 7 T at a current of 200 A with a field uniformity of 0.24%. Next, the magnet was consistently operated in the persistent-mode at the 7 T field for 9.5 days. During persistent-mode operation, the magnet achieved a magnetic field decay rate of 0.42 ppm · h^{-1}, which is reliable performance for practical application. Based on the results, our magnet is capable of providing stable, long-term operation for generating HCIs in EBISs.

REFERENCES

[1] G. Zschornack, F. Grossmann, U. Kentsch, V. P. Ovsyannikov, E. Ritter, M. Schmidt, A. Thorn, and F. Ullmann, "Status report of the Dresden EBIS/EBIT developments," *Rev. Sci. Instrum.*, vol. 81, no. 2, Feb. 2010, Art. no. 02A512, doi: 10.1063/1.3267846.

[2] G. Zschornacka, M. Schmidt, and A. Thorn, "Electron beam ion sources," CERN, Geneva, Switzerland, Tech. Rep. CERN-2013-007, 2014.

[3] S. Lee, H. S. Kim, H. J. Kwon, and Y. S. Cho, "Characterization of EBIS test bench at KOMAC," in *Proc. AIP Conf.*, 2018, pp. 3–6, doi: 10.1063/1.5053283.

[4] S. Lee, H. S. Kim, H. J. Kwon, and Y. S. Cho, "Implementation and preliminary test of electron beam ion sources at KOMAC," in *Proc. 7th Int. Part. Accel. Conf. (IPAC)*, 2016, pp. 1311–1313, doi: 10.18429/JACoW-IPAC2016-TUPMR031.

[5] U. Kentsch, G. Zschornack, A. Schwan, and F. Ullmann, "Short time ion pulse extraction from the Dresden electron beam ion trap," *Rev. Sci. Instrum.*, vol. 81, no. 2, 2010, Art. no. 02A507, doi: 10.1063/1.3271255.

[6] M. Schmidt, H. Peng, G. Zschornack, and S. Sykora, "A compact electron beam ion source with integrated Wien filter providing mass and charge state separated beams of highly charged ions," *Rev. Sci. Instrum.*, vol. 80, no. 6, Jun. 2009, Art. no. 063301, doi: 10.1063/1.3125628.

[7] Y.-H. Park, H.-J. Son, and J. Kim, "Design of an EBIS charge breeder system for rare-isotope beams," *J. Korean Phys. Soc.*, vol. 69, no. 6, pp. 962–966, Sep. 2016, doi: 10.3938/jkps.69.962.

[8] A. Shornikov and F. Wenander, "Advanced electron beam ion sources (EBIS) for 2-nd generation carbon radiotherapy facilities," *J. Instrum.*, vol. 11, no. 4, Apr. 2016, Art. no. T04001, doi: 10.1088/1748-0221/11/04/T04001.

[9] B. Wolf, *Handbook of Ion Sources*. Boca Raton, FL, USA: CRC Press, 2017.

[10] S. Cho, J. Kim, Y. Song, L. Seunghyun, and H. Kim, "Implementation of EBIS control system for a pulsed neutron source at KOMAC," *Trans. Korean Nucl. Soc. Virtual Spring Meeting*, pp. 9–11, Mar. 2020.

[11] S. Lee, H. Kwon, H. Kim, and Y. Cho, "Installation, commissioning and characterization of EBIS-SC as a short pulsed proton source at KOMAC," in *Proc. 9th Int. Part. Accel. Conf. (IPAC)*, 2018, pp. 1721–1723, doi: 10.18429/JACoW-IPAC2018-TUPML076.

[12] J. G. Alessi, D. Barton, E. Beebe, and S. Bellavia, "The Brookhaven national laboratory electron beam ion source for RHIC," *Rev. Sci. Instrum.*, vol. 81, no. 2, Feb. 2010, Art. no. 02A509, doi: 10.1063/1.3292937.

[13] S. Kondrashev, A. Barcikowski, and C. Dickerson, "EBIS charge breeder for CARIBU," *Rev. Sci. Instrum.*, vol. 85, no. 2, Feb. 2014, Art. no. 02B901, doi: 10.1063/1.4824645.

[14] S. Kondrashev, C. Dickerson, and A. Levand, "Commissioning of CARIBU EBIS charge breeder sub-systems," in *Proc. 12th Heavy Ion Accel. Technol. Conf. Chicago*, 2012, pp. 165–169.

[15] J. Zhu, Y. Ren, F. Wang, W. Chen, and Z. Chen, "A homogeneous superconducting magnet system for EBIT," *IEEE Trans. Appl. Supercond.*, vol. 24, no. 4, Aug. 2014, Art. no. 4901404, doi: 10.1109/TASC.2014.2311406.

[16] D. Kramer, "Helium users are at the mercy of suppliers," *Phys. Today*, vol. 72, no. 4, pp. 26–29, Apr. 2019, doi: 10.1063/PT.3.4181.

[17] Z. Wang, J. M. van Oort, and M. X. Zou, "Development of superconducting magnet for high-field MR systems in China," *Phys. C: Supercond. Appl.*, vol. 482, pp. 80–86, Nov. 2012, doi: 10.1016/j.physc.2012.04.027.

[18] Y. Lvovsky, E. W. Stautner, and T. Zhang, "Novel technologies and configurations of superconducting magnets for MRI," *Supercond. Sci. Technol.*, vol. 26, no. 9, Sep. 2013, Art. no. 093001, doi: 10.1088/0953-2048/26/9/093001.

[19] S.-H. Kim, S.-H. Lee, D. Patel, and S. Choi, "A cryogen recondensing cooling system for a 7 T superconducting solenoid magnet in an electron beam ion source system," *IEEE Trans. Appl. Supercond.*, vol. 28, no. 3, pp. 1–4, Apr. 2018, doi: 10.1109/TASC.2018.2794341.

[20] Cryomagnetics. (Mar. 1, 2018). *Electron Beam Ion Source (EBIS)*. Accessed: Aug. 31, 2021. [Online]. Available: https://www.cryomagnetics.com/electron_beam_ion_source_ebis/

[21] A. Berryhill and J. Ritter, "A dual 5T superconducting magnet system for the brookhaven national lab electron beam ion source," *IEEE Trans. Appl. Supercond.*, vol. 29, no. 5, Aug. 2019, Art. no. 4100104, doi: 10.1109/TASC.2019.2892064.

[22] D. Patel, S.-H. Kim, W. Qiu, M. Maeda, A. Matsumoto, G. Nishijima, H. Kumakura, S. Choi, and J. H. Kim, "Niobium-titanium (Nb-Ti) superconducting joints for persistent-mode operation," *Sci. Rep.*, vol. 9, no. 1, pp. 1–7, Dec. 2019, doi: 10.1038/s41598-019-50549-7.

[23] Luvata. (2018). *Superconductors*. Accessed: Aug. 31, 2021. [Online]. Available: https://www.luvata.com/products/superconductors

[24] Y. Iwasa, *Case Studies in Superconducting Magnets*, 2nd ed. Boston, MA, USA: Springer, 2009.

[25] D. B. Montgomery, *Solenoid Magnet Design: The Magnetic and Mechanical Aspects of Resistive and Superconducting Systems*. New York, NY, USA: Wiley, 1969.

[26] J. Ekin, *Experimental Techniques for Low-Temperature Measurements: Cryo-Stat Design, Material Properties and Superconductor Critical-Current Testing*. Oxford, U.K.: Oxford Univ. Press, 2006.

[27] M. Guan, X. Wang, and Y. Zhou, "The influence of strain rate on the tensile properties of a Nb–Ti/Cu superconducting composite wire under variable cryogenic temperature," *IEEE Trans. Appl. Supercond.*, vol. 26, no. 2, Mar. 2016, Art. no. 8400205, doi: 10.1109/TASC.2015.2510608.

[28] P. Kittel, *Advances in Cryogenic Engineering*. Boston, MA, USA: Springer, 1994.

[29] SUPERCON. (2015). *CuNi Resistive Wires*. Accessed: Aug. 31, 2021. [Online]. Available: http://www.supercon-wire.com/content/cuni-resistive-wires
[30] M. N. Wilson, *Superconducting Magnets*. Oxford, U.K.: Clarendon Press, 1987.
[31] D. Patel, M. S. Al Hossain, A. Motaman, S. Barua, M. Shahabuddin, and J. H. Kim, "Rational design of MgB_2 conductors toward practical applications," *Cryogenics*, vol. 63, pp. 160–165, Sep./Oct. 2014, doi: 10.1016/j.cryogenics.2014.04.016.

SU-HUN KIM (Member, IEEE) received the bachelor's degree from Paichai University, South Korea, in 2012, the master's degree from Sungkyunkwan University, South Korea, in 2014, and the Ph.D. degree from Kyungpook National University, South Korea, in 2020. He is currently a Postdoctoral Researcher with the Department of Electrical Engineering, Kyungpook National University. His research interests include superconducting magnet and joint for application and electromagnetic muliphysics system design.

DIPAK PATEL received the bachelor's degree from Hemchandracharya North Gujarat University, India, in 2005, the master's degree from Annamalai University, India, in 2010, and the Ph.D. degree from the University of Wollongong, Australia, in 2016. He is currently a Postdoctoral Research Fellow with the School of Mechanical and Mining Engineering, University of Queensland, Australia. His research interests include superconducting materials and their magnet applications.

YEUNDAE JEONG received the bachelor's degree from Korea Aerospace University, South Korea, in 1998. He is currently a Technical Director at KR Tech, South Korea. His research interests include superconducting magnet design and its application.

MINHEE KIM received the bachelor's degree from Sungkyunkwan University, South Korea, in 2012, and the master's and Ph.D. degrees from Kyungpook National University, South Korea, in 2019 and 2022, respectively. She is currently a Postdoctoral Researcher with the School of Electronic and Electrical Engineering, Kyungpook National University. Her research interests include electromagnetic multiphysics system analysis for application.

SE-HEE LEE received the bachelor's and master's degrees from Soongsil University, South Korea, in 1996 and 1998, respectively, and the Ph.D. degree from Sungkyunkwan University, South Korea, in 2002. He is currently a Professor with the School of Electronic and Electrical Engineering, Kyungpook National University, South Korea. His research interests include analysis and design for electromagnetic multiphysics problems spanning the macro- to the nano-scales.

JUNG HO KIM received the bachelor's, master's, and Ph.D. degrees from Sungkyunkwan University, South Korea, in 1998, 2000, and 2005, respectively. He is currently a Professor with the Australian Institute for Innovative Materials (AIIM), University of Wollongong, Australia. His research interest includes superconducting material.

SEYONG CHOI received the bachelor's, master's, and Ph.D. degrees in electrical engineering from Sungkyunkwan University, South Korea, in 1998, 2000, and 2005, respectively. He is currently an Assistant Professor with the Department of Electrical Engineering, Kangwon National University, South Korea. His research interest includes applied superconductivity and its application employing superconducting magnet.